

# Performance Evaluation on Wireless Communication Technology for Implantable Wireless Body Area Network

Kenichi Takizawa<sup>a</sup>, Takahiro Aoyagi<sup>a</sup>, Kiyoshi Hamaguchi<sup>a</sup>, and Ryuji Kohno<sup>a</sup>

<sup>a</sup> National Institute of Information and Communications Technology (NICT), Yokosuka, Japan

## Abstract

This paper presents a performance evaluation of a wireless implantable body area network by using a model on received signal strength (RSS), which represents channel quality between implanted and on-body devices. In order to derive the statistical model, we carried out a measurement on RSS by using small-size signal generator, small-size chip antenna, and liquid phantom. RSS is measured at various distances to obtain a statistical model which gives RSS for a distance between implanted and on-body antennas. Statistical models are given for the frequency bands of 403, 611, 953, and 2450 MHz. By using the models, a cumulative distribution function on received SNR for each frequency is obtained. The results show that the frequency bands of 953 and 2450 MHz give marginal link margin when we use GFSK modulation as wireless communications. Also, we show that the received SNR is improved by introducing multiple antennas which are attached around the human body.

**Keywords:** *Wireless body area networks (WBANs), Implants, Channel modeling, GFSK*

## Introduction

In medical applications, the use of a wireless communication technology has been paid attention in order to successfully reduce both workload and economic costs without the decrease of quality of medical treatments. Wireless communication technologies are typically categorized from the viewpoint of the size of coverage area. The first category is wide-area communication technologies, in which WiMAX [1] and cellular phone are included. The wireless communication technologies in this category are available to provide wireless link between terminal devices for tele-monitoring in medical applications [2]. Another category is middle-area technologies such as WiFi [3], which provides wireless connection over a couple of hospital rooms by a single AP [4]. And, the other one is short-range communications such as Bluetooth [5], Zigbee [6], WiMedia [7], and so on. In the category of short-range communications, wireless body area network (WBAN) is a new class of wireless communication technologies. WBAN provides wireless connection between implanted devices and devices on and around human body. Such wireless technology, named as implantable WBAN, enables to monitor

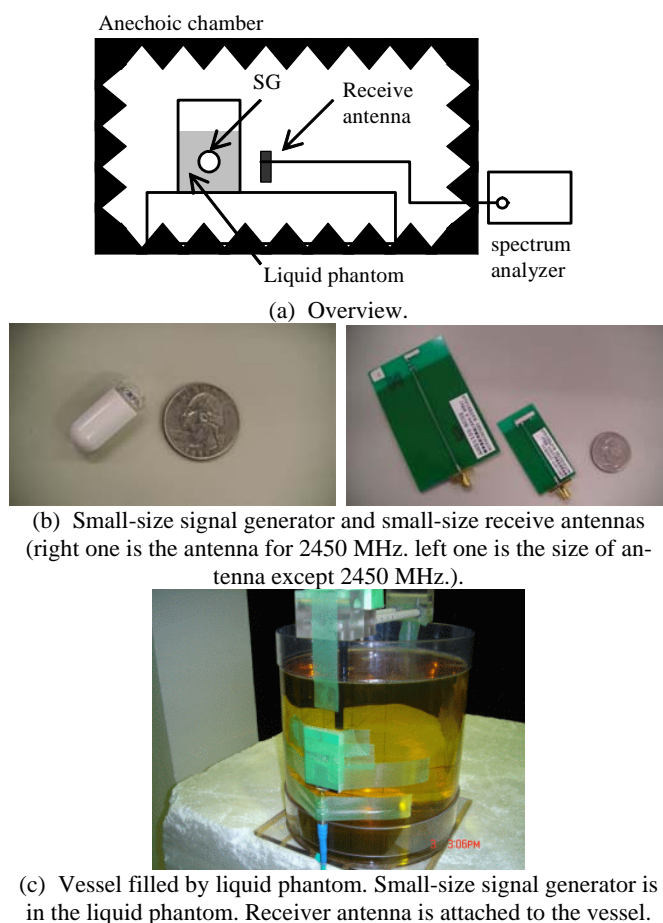


Figure 1. Measurement setup.

in-vivo vital signs [11], video of a digestive system [12], and various kinds of in-vivo physiological data.

On the design of a radio communication technology for such implantable WBAN, the first step is to decide the frequency band. Based on the current international radio regulation, there is a frequency band for medical implantable communication systems (MICS) [8]. The frequency band ranges from 402 to 405 MHz. MICS is suitable band to provide wireless peer-to-peer communications for low-rate and low-duty data transmission. However, there are limitations on the use of MICS in duty cycle, bandwidth, radiation level, transmission protocol, and so on. Several applications using implanted de-

Table 1. Complex permittivity of the liquid phantom

Frequency [MHz]	$\epsilon'$	$\epsilon''$
403	42.27	39.40
611	40.20	29.78
953	37.28	23.04
2450	31.00	17.98

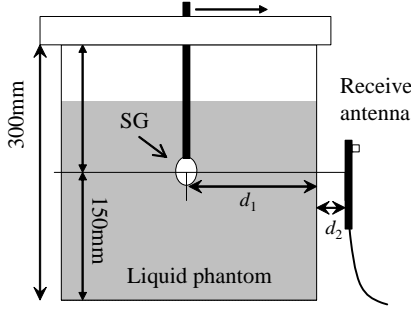


Figure 2. Measurement procedure by setting the signal generator at distance  $d_1$  from 50 to 150 mm by 20 mm.

vices such as capsule endoscope require wider bandwidth of more than a couple of Mbps. Another candidate of available frequency bands is industrial, scientific, and medical (ISM) band, which ranges from 2400 to 2483 MHz. In the North America, 950-MHz band is also available. In addition to MICS and ISM, 611-MHz band is also available as wireless medical telemetry service (WMTS) [9] in the United States. These frequency bands of MICS (403MHz), ISM (950MHz and 2450 MHz), and WMTS (611MHz) are candidates for implantable WBAN; however, no comparison among such frequency bands from the viewpoint of the design of radio communications for implantable WBAN has been reported.

This paper presents a model on received signal strength (RSS) and shows performance evaluation by using the obtained model for the frequency bands of 403, 611, 953, and 2450 MHz. These models are derived from measured RSS in a setup assuming capsule endoscope application. In this setup, a small-size signal oscillator, chip antenna as receive antenna, and liquid phantom are used. Performance evaluation on Gaussian filtered frequency shift keying (GFSK)-based wireless communication system is shown by using the statistical RSS model. GFSK [10] is a good candidate for implantable WBAN since the operation under low-power consumption is expected.

## Model of received signal strength

### Overview

A statistical model to show quality of wireless channel is essential to evaluate wireless communications. We derive a model of RSS corresponding to the transmission distance within the liquid phantom. In order to obtain such statistical model, a measurement based on a usage model of capsule endoscope is carried out for the frequency bands of 403, 611, 953, and 2450 MHz.

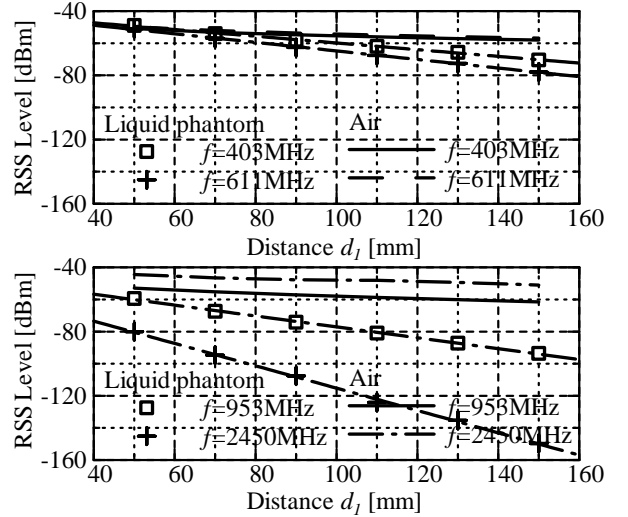


Figure 3. Dependency of the Measured RSS levels to distance  $d_1$  in each frequency (403, 611, 953, and 2450 MHz).

Table 2. Parameters' values of the model on the RSS level

Frequency $f$ [MHz]	Coefficients	Correlation coefficient
403	$a(f) = -0.21, b(f) = -38.95$	0.999
611	$a(f) = -0.27, b(f) = -38.12$	0.999
953	$a(f) = -0.34, b(f) = -43.17$	0.999
2450	$a(f) = -0.69, b(f) = -45.66$	0.999

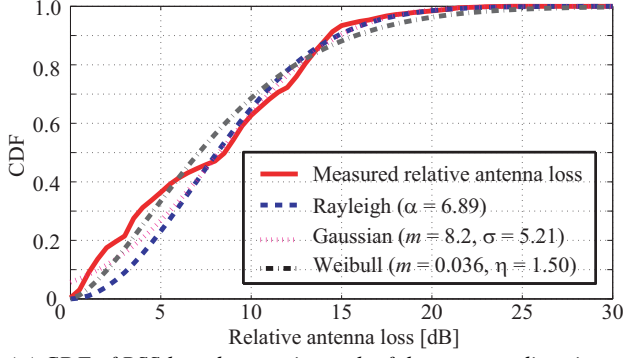
### Measurement setup

Measurement setup is shown in Fig. 1. This measurement is conducted in an anechoic chamber. A signal generator radiates a radio frequency continuous wave (CW) at one of the frequencies. RSS level is measured by a spectrum analyzer received by an antenna. An amplifier is inserted before the spectrum analyzer. The gain of this amplifier and losses of cables are compensated after the measurement. The size of the signal generator is 18 mm in the length and 10 mm in the diameter. Liquid phantom in a cylinder-shape vessel has electrical constants as shown in Table 1. The radius of this vessel is 150 mm. The receive antennas are placed on the vessel. A receiver antenna is prepared for each frequency. The antennas provide gain of 0 dBi and omni-directional pattern in the horizontal plane in free space. During the measurement, SG is set as to face the direction of the maximum gain with the receive antenna.

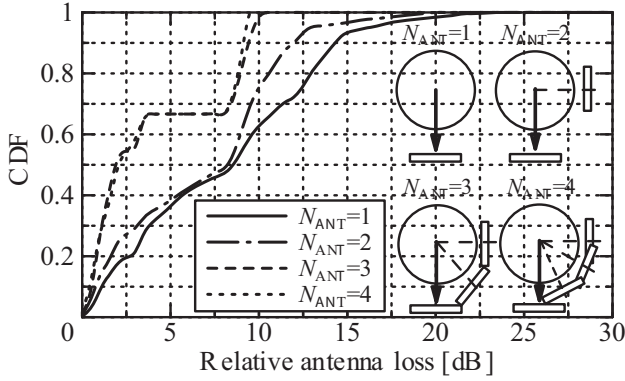
As shown in Fig.2, RSS is measured in distances in the liquid phantom, denoted by  $d_1$ , from 50 mm to 150 mm by 20 mm. The distance between the vessel and receive antenna, denoted by  $d_2$ , is fixed to 15 mm. The thickness of the vessel is 2 mm, and the vessel is made by polycarbonate.

### Measurement results and a model of RSS

Fig. 3 summarizes measured RSS levels and fitting results through least square fitting. As a reference, measured RSS in free space are also plotted. The measured results show that the attenuation due to the liquid phantom increases as the frequency of CW increases. For example, at the distance  $d_1$  of 90 mm and  $d_2$  of 15 mm, RSS level at 403 MHz and 2450 MHz is -58.1 and -107.8 dBm, respectively. The level at 403 MHz



(a) CDF of RSS loss due to mismatch of the antenna directions, denoted as relative antenna loss, are shown and fitted by Rayleigh, Gaussian, and Weibull distributions.



(b) CDF of relative loss in the use of multiple antennas.

Figure 4. Statistical model of relative antenna loss.

is superior by more than 50 dB to that at 2450 MHz. Thus, even though higher RF radiation is permitted in the 2.4-GHz ISM band, link margin of the use of 2.4 GHz will be marginal. Based on the measurement results, a statistical model on RSS is derived. A model which gives RSS level for the distance  $d_1$  is simply expressed by a linear curve shown below.

$$\text{RSS}(d_1, f) [\text{dBm}] = a(f) \cdot d_1 [\text{mm}] + b(f) \quad (1)$$

where the coefficients  $a(f)$  and  $b(f)$  are determined by a least square fitting. The values of the coefficients for each frequency  $f$  are summarized in Table 2. By using this model, evaluation of probability distribution on RSS is realized by introducing a probability distribution of the distance in human tissue.

## Performance evaluation of implantable WBAN

Statistical distribution of signal-to-noise ratio (SNR) at the receive antenna is shown. Also, bit error ratio (BER) and packet error ratio (PER) of GFSK are also given to determine the SNR to provide required BER or PER. In this performance evaluation, we focus on usage model of capsule endoscope as implanted WBAN application. So, firstly, in order to evaluate the performance based on the capsule endoscope application, statistical models on both RSS loss due to mismatch on the directions between implanted and on-body antennas and the propagation distance in human tissue are derived.

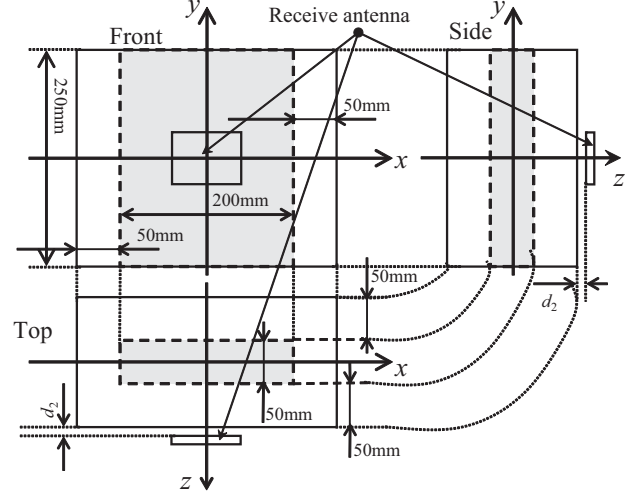


Figure 5. A human-body model for obtaining a statistical distribution of the propagation distance. We assume that an implanted device move the colored part uniformly.

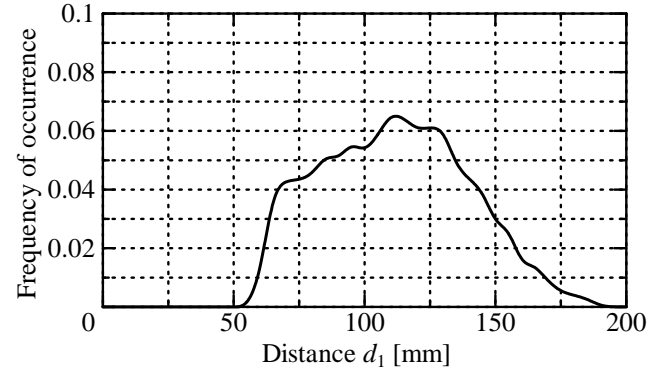


Figure 6. Histogram of propagation distance  $d_1$  for the human-body model shown in Figure 5.

## Statistical model of RSS loss due to mismatch of antenna directions between implanted and on-body devices

In the measurement of RSS levels in the anechoic chamber, the direction providing the maximum radiation of the signal generator faces the receive antenna. However, in real situations, a mismatch of antenna's directions causes loss in the RSS level. Here, a loss due to change of the implanted device's direction is modeled. In order to obtain a statistical model on the loss, cumulative distribution function (CDF) on relative antenna at the implanted device is shown in Fig. 4(a). CDF curve is obtained by measuring antenna gain over the x-y, y-z, and z-x planes. The relative antenna loss is the measured antenna gain normalized by the maximum gain of this antenna. In the measurement of RSS levels, the maximum gain of the implanted device's antenna faced with the receive antenna. Thus, the fluctuation of RSS level due to the change of the direction at the implanted devices is obtainable by introducing the CDF shown in Fig. 4(a). CDF curve on the relative antenna loss is fitted by Weibull, Rayleigh, and Gaussian distributions. As a result, Weibull distribution with parameters  $m$  of 0.036 and  $\eta$  of 1.50 provides the best correlation with the original CDF. Thus, probability density function (PDF) of the relative antenna loss  $l_{\text{ANT}}$ , which is modeled by Weibull

distribution, is given by

$$p(l_{\text{ANT}}) = \frac{m}{\eta} \left( \frac{l_{\text{ANT}}}{\eta} \right)^{m-1} \exp \left\{ - \left( \frac{l_{\text{ANT}}}{\eta} \right)^m \right\} \quad (2)$$

The plot shown in Fig. 4(a) also tells us that a single-antenna system probably fall in deep fade like RSS level of less than -100 dBm. In this case, it is hard to connect a wireless link between implantable and outside-body devices. In order to avoid such deep fade on RSS level, a simple approach is to introduce a multiple antenna system, in which relative antenna loss for an angle is able to be compensated by another antenna set at another angle. Based on selection diversity approach, the relative loss  $l_{\text{MULTI\_ANT}}$  for an angle  $\theta$  is written as

$$l_{\text{MULTI\_ANT}}(\theta) = \min_{i=1, \dots, N_{\text{ANT}}} \left\{ l_{\text{ANT}} \left( \theta + (i-1) \cdot \frac{\pi}{2 \cdot N_{\text{ANT}}} \right) \right\} \quad (3)$$

In this equation, we assume that all of antennas are attached in the same plane as shown in Fig. 4(b), in which CDFs for multiple-antenna systems with the various numbers of antennas  $N_{\text{ANT}}$  are also shown. As the number of antennas increases, slope of CDF on the relative antenna loss becomes sharp. However, the CDF with  $N_{\text{ANT}}$  of 3 and that with  $N_{\text{ANT}}$  of 4 is comparable. So, in our performance evaluation, the number of antennas is set to up to 3. PDF for a multiple-antenna system,  $p(l_{\text{ANT\_MULTI}})$ , is obtained by a least-square fitting in Weibull distribution as same as the single-antenna system.

#### Statistical model of propagation distance in capsule endoscope application

A propagation distance  $d_1$  is modeled by using a simple cubic model shown in Fig.5. The target application is capsule endoscope for small intestine. So, we assume an implanted device moves in the colored part uniformly. This part has height (y-axis) of 250 mm, width (x-axis) of 200 mm, and depth (z-axis) of 50 mm. There is a 50-mm distance between the body surface and the colored part. On the derivation of the propagation distance, it is assumed that an outside-body antenna is fixed at distance of  $d_2$  from the surface of the model. Based on this model, the histogram of the propagation distances  $d_1$  is obtained. The histogram is shown in Fig. 6. The propagation distance ranges from 50 mm to 200 mm, and the most frequent distance is 135 mm. This histogram is used as discrete probability distribution function of the distance  $d_1$ , denoted as  $p(d_1)$ .

#### Cumulative distribution of received SNR

By using the derived models on its RSS level for the propagation distance, relative antenna loss, and propagation distance, we estimate received SNR distribution. The received SNR determines error rate performance of wireless communication technologies. The average SNR for one of the measured frequency  $f$  is given by

$$\text{SNR}(f) = \iint \{ \text{RSS}(d_1, f) - l_{\text{ANT}} - N(f) \} p(d_1) p(l_{\text{ANT}}) dd_1 dl_{\text{ANT}} \quad (4)$$

where  $N(f)$  denotes the noise level given by  $kTBN_f$  for frequency  $f$ . If a multi-antenna system is introduced,  $l_{\text{ANT}}$  in Eq.(4) is replaced by  $l_{\text{ANT\_MULTI}}$ . The noise figure  $N_f$  is set to 7 dB. The PDF of the received SNR is numerically obtained by

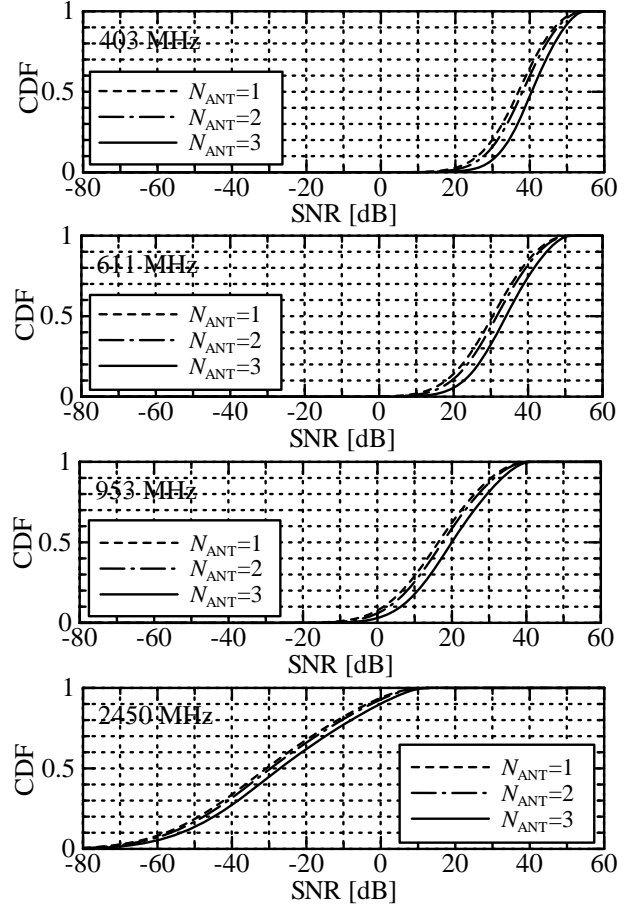


Figure 7. CDF of the received SNR for each frequency in single and multiple antenna systems.

$$p(\text{SNR}(f)) = p(d_1) \otimes p(l_{\text{ANT}}) \quad (5)$$

And, CDF of the received SNR is obtained from Eq. (5). The derived CDF is shown in Fig. 7. The frequency band of 2450 MHz provides no positive SNR. On the other hand, the CDFs in 403 and 611 MHz show a link margin enough to maintain a wireless connection link, which is important for medical applications since highly reliable connection is required. The 953-MHz band gives partly positive SNR. The CDF also shows that the use of a multiple-antenna system brings SNR improvement.

#### BER and PER performance

In performance evaluation of wireless communications, BER and PER performance are evaluated in average value in general. However, medical applications require a highly reliable wireless connection. So, we employ an outage evaluation instead of average evaluation in the error rate performance. The  $P$ -% outage values is defined as

$$\int_{-\infty}^{\text{SNR}_{P\%}(f)} p(\text{SNR}(f)) d\text{SNR} = P \times 10^{-2} \quad (4)$$

Thus,  $\text{SNR}_{P\%}(f)$  means that the receiver can capture SNR more than  $\text{SNR}_{P\%}(f)$  with the probability of  $P$  %. For  $P = 90, 99, \text{ and } 99.9$ , the outage values are calculated in both single and multiple antenna systems. The calculated results are

Table 3. Outage values of the received SNR in decibel for 90, 99, and 99.9 % in each frequency band.

Frequency $f$ [MHz]	SNR <sub>90%</sub>	SNR <sub>99%</sub>	SNR <sub>99.9%</sub>
403	26.0 ( $N_{ANT}=1$ )	16.5 ( $N_{ANT}=1$ )	9.5 ( $N_{ANT}=1$ )
	28.0 ( $N_{ANT}=2$ )	18.5 ( $N_{ANT}=2$ )	11.0 ( $N_{ANT}=2$ )
	31.5 ( $N_{ANT}=3$ )	22.5 ( $N_{ANT}=3$ )	15.0 ( $N_{ANT}=3$ )
611	18.0 ( $N_{ANT}=1$ )	7.5 ( $N_{ANT}=1$ )	0.0 ( $N_{ANT}=1$ )
	19.5 ( $N_{ANT}=2$ )	9.5 ( $N_{ANT}=2$ )	2.0 ( $N_{ANT}=2$ )
	23.0 ( $N_{ANT}=3$ )	13.5 ( $N_{ANT}=3$ )	6.0 ( $N_{ANT}=3$ )
953	2.0 ( $N_{ANT}=1$ )	-10.0 ( $N_{ANT}=1$ )	-18.0 ( $N_{ANT}=1$ )
	3.5 ( $N_{ANT}=2$ )	-8.0 ( $N_{ANT}=2$ )	-16.0 ( $N_{ANT}=2$ )
	6.0 ( $N_{ANT}=3$ )	-4.0 ( $N_{ANT}=3$ )	-12.0 ( $N_{ANT}=3$ )
2450	-57.5 ( $N_{ANT}=1$ )	-77.0 ( $N_{ANT}=1$ )	-88.0 ( $N_{ANT}=1$ )
	-76.5 ( $N_{ANT}=2$ )	-75.5 ( $N_{ANT}=2$ )	-86.0 ( $N_{ANT}=2$ )
	-53.5 ( $N_{ANT}=3$ )	-72.5 ( $N_{ANT}=3$ )	-82.0 ( $N_{ANT}=3$ )

summarized in Table 3. In the 403 MHz, even in  $P = 99.9$ , the outage received SNR is more than 9.5 dB. On the other hand, there is no positive SNR in 2450 MHz frequency band.

As mentioned in the introduction, we use GFSK modulation as radio communication for implantable WBAN. Fig. 8 shows bit and packet error ratio of GFSK. The horizontal axis,  $E_b/N_0$ , indicates the SNR per information bit. The packet size is set to 128 Bytes. Its modulation index  $m$  and BT are set to 1.0 and 0.5, respectively. Setting target PER of  $10^{-2}$ , the required SNR is 16.1 dB. Thus, the use of 403 MHz signal brings 99-% probability on the successful wireless transmission using the GFSK with single antenna. In the 611 MHz, the outage probability of the successful wireless connection is 90 %. Both 953- and 2450-MHz bands can not provide received SNR in outage probability of more than 90 %.

## Conclusion

This paper presents a performance evaluation of wireless communication technology for implantable WBAN. The measurement results on RSS from a small-size SG put into a liquid phantom are used to model its RSS level for propagation distance in the liquid phantom. We also provided antenna loss and propagation distance models. By using these models, we showed CDF of the received SNR and outage values for 90, 99, and 99.9 % are shown. Computer simulation was carried out to evaluate error rate performance for a GFSK-based wireless communication system. The results show that both 403- and 611-MHz bands provide link margin enough to establish a wireless connection by using multiple-antenna system.

## Acknowledgments

The authors thank to Prof. Takehiko Kobayashi, Prof. Jun-ichi Takada, Dr. Shinobu Ishigami, and Dr. Lira Hamada for their useful comments to the experiments.

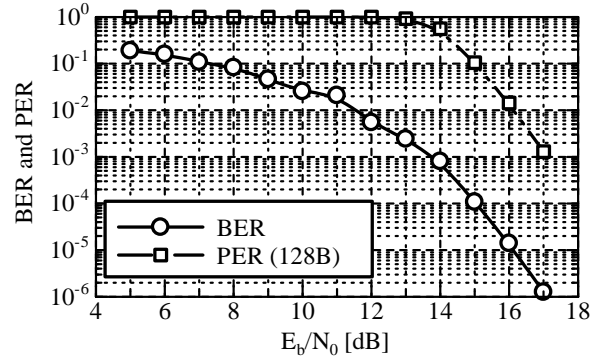


Figure 8. BER and PER performance of GFSK in modulation index of 1.0 and BT of 0.5.

## References

- [1] B. Li, Y. Qin, C. P. Low, and C. L. Gwee, "A Survey on Mobile WiMAX," IEEE Communications Magazine, Vol. 45, No. 12, pp. 70-75, Dec. 2007.
- [2] R. Istepanian, "WiMAX For Mobile Healthcare Applications," WiMax London 2007, pp. 1-43, Apr. 2007.
- [3] WiFi Alliance, <http://www.wi-fi.org/>.
- [4] J. Jiang, Z. Yan, and J. Shi, "The Design of Medical Assistant System for Ward Doctors," Proc. of the 3rd IEEE/EMBS International Summer School on Medical Devices and Biosensors, pp. 109-111, Sept. 2006.
- [5] Y. Zheng and Z. Feng, "Simplifications of the Bluetooth radio devices," Proc. of IEEE 4th International Workshop on Networked Appliances, pp. 107-115, 2002.
- [6] ZigBee Alliance, ZigBee Specification Version 1.0, <http://www.zigbee.org>, December 14th, 2004.
- [7] N. Kumar and R.M. Buehrer, "The ultra wideband WiMedia standard," IEEE Signal Processing Magazine, Vol. 25, No. 5, pp. 115-119, Sept. 2008.
- [8] H.S. Savci, A. Sula, Z. Wang, N.S. Dogan, and E. Arvas, "MICS transceivers: regulatory standards and applications," Proc. of IEEE SoutheastCon 2005, pp. 179-182, Apr. 2005.
- [9] FCC Rules and Regulations, "WMTS Band Plan," Part 95, Mar. 2003.
- [10] J. G. Proakis, Digital communications 4th edition, McGrawHill.
- [11] M. R. Yuce, S. W. P. Ng, N. L. Myo, C. K. Lee, J. Y. Khan, and W. Liu, "A MICS Band Wireless Body Sensor Network," Proc. of IEEE Wireless Communications and Networking Conference(WCNC) 2007, pp. 2473-2478, Mar. 2007.
- [12] M.Q.-H. Meng, M. Tao, J. Pu, C. Hu, X. Wang, and Y. Chan, "Wireless robotic capsule endoscopy: state-of-the-art and challenges," Proc. of Fifth World Congress on Intelligent Control and Automation (WCICA) 2004, Vol. 6, pp. 5561-5565, June 2004.